Photodissociation of NO$_2$ in the Region 217−237 nm: Nascent NO Energy Distribution and Mechanism[†]

H.-S. Im and E. R. Bernstein*

Department of Chemistry, Colorado State University, Fort Collins, Colorado 80523-1872

Received: October 25, 2001; In Final Form: May 22, 2002

Photodissociation of NO$_2$ in the region of 217−237 nm is investigated by probing the nascent NO generated using a one-laser photofragmentation/fragment-detection technique. By mixing O$_2$ in the sample (20%−100%) and by setting proper detection timing, only mass-resolved excitation spectra (MRES) of photofragmented NO are obtained and examined. The nascent NO spectrum changes depending on the intensity (W/cm^2) of the laser beam. For low laser intensity, the dissociation of NO$_2$ produces rotationally and vibrationally cold NO through the NO$_2$ 2^{2}B$_2$ (B̃) excited state. Excess energy for this photofragmentation is ∼0.4 eV at 226 nm. This excess energy is distributed almost entirely to the kinetic energy of NO(X ^{2}A$_2$) and O(^{1}D) products. The spectrum of photofragmented NO becomes very crowded as the laser intensity is increased because higher rotational and vibrational levels of NO become populated through multiphoton excitation and eventual photofragmentation of NO$_2$ from higher-energy electronic states. The rotational temperature of NO is ca. 200 K for high laser intensity and less than 30 K for low laser intensity. Near 230 nm, a rovibronic spectrum is observed that cannot be attributed to NO even though it is detected in the NO mass channel. The time-of-flight mass spectrum line width for photofragmented NO in this photolysis region increases by a factor of 2 to about 40 ns (estimated NO kinetic energy is 0.40 ± 0.04 eV) for high laser intensity. These observations lead to the conclusion that a higher electronic state of NO$_2$ has been accessed to generate highly excited NO through multiphoton absorption processes for the high laser intensity experiments. Such intermediate states can be Rydberg, ion pair, or other high-energy states of NO$_2$ accessed by multiphoton absorption.

I. Introduction

The NO$_2$ molecule appears as an important component of combustion systems, atmospheric chemistry, and energetic materials decomposition. Spectroscopy and photofragment dynamics studies of NO$_2$ have revealed a very rich and varied set of molecular properties for this triatomic molecule. Sufficiently strong intramolecular vibration, rotation, and electronic-state interactions exist in this molecule that the visible region of the spectrum of NO$_2$ displays apparently chaotic dynamics and over 10^3 resolvable features.[1] Photodissociation of NO$_2$ to give NO + O has been studied as a model of unimolecular fragmentation dynamics. As new spectroscopic and photodissociation methods have become available in the last 30 years, they have systematically been applied to this prototypic system.[2] Such NO detection of nitro compound (RNO$_2$) photofragmentation has been employed for an analysis/detection technique for fuels and explosives.

The photochemistry of NO$_2$ has been studied extensively for many years, with particular attention given to the first dissociation threshold (NO$_2$ + $h\nu$ (∼2.5 × 10^4 cm^{-1}) → NO(X $^2\Pi$) + O(^{3}P))[3], and various photon energies have been utilized.[4] A few studies[5] are carried out near 4.0 × 10^4 cm^{-1}. These studies have focused on the characterization of NO internal and external energy distributions. Recently, femtosecond laser excitation at 2.7 × 10^4 cm^{-1} photon energy has been employed to study the dissociation and competitive ionization of NO$_2$.[6] These various excitation energies are not high enough to open the O(^{1}D) dissociation channel: O(^{1}D) can only appear above 5.08 eV

(40 995 cm^{-1} or 244 nm). At lower energies than this latter value, the excess reaction energy must go into NO rotations, vibrations, product translational energy, spin−orbit levels (Ω) of NO($^2\Pi_\Omega$; v, J), or internal states of O(^{3}P$_j$) or a combination thereof. Experimental conditions, such as laser intensity, laser wavelength, and detection method, can have significant consequences for NO$_2$ photodissociation studies. For example, photolysis of NO$_2$ at 248 nm (40 323 cm^{-1}) monitored by laser-induced fluorescence (LIF) of NO is reported to yield nascent NO with a strongly inverted population with a maximum at $v'' = 6-8$ and no population in $v'' = 0$.[5a] Another study under ostensibly the same experimental conditions but employing resonance-enhanced multiphoton ionization (REMPI) for detection of nascent NO, however, determined that the vibrational distribution of NO peaks at $v'' = 5$ and has a large $v'' = 0$ population.[5b]

Photodissociation of NO$_2$ at higher energies has also been studied. The 2 ^{2}B$_2$ (B̃) origin is at $T_0 = 40\,126$ cm^{-1}, and at 40 972 cm^{-1} ($T_0 + \sim850$ cm^{-1}), the NO$_2$ → NO(X) + O(^{1}D) channel opens. Morrison and Grant[7] studied the dynamics of NO$_2$ dissociation via this high-energy B̃ state using two-photon photodissociation with visible light. They concluded that the internal energy distribution in the nascent NO produced by this two-photon O(^{1}D) pathway qualitatively resembles that observed for the one-photon dissociation via the O(^{3}P) pathway for similar excess energies. Bigio et al.[8] have studied single-photon photodissociation of NO$_2$ to compare the dynamics of one-photon vs isoenergetic two-photon photodissociation. They report the spectrum of photofragmented NO using a focused high-intensity laser beam in the region 227−220 nm. A

7566 *J. Phys. Chem. A, Vol. 106, No. 33, 2002*

Im and Bernstein

simulation of rotational distribution characterizing the spectra of ref 8 yields a rotational temperature of ca. 200−300 K. Marshall et al.[9] demonstrate that the spectrum of NO obtained from NO_2 is different than that found for NO gas itself. At 232 nm, they observed a band in the NO-detected NO_2 photofragmentation spectrum that is not present in the NO spectrum.

Other experiments explore NO_2 fragmentation behavior through observation of the O atom states using one- or two-photon laser-induced fluorescence (LIF),[10] REMPI,[11] and ion imaging.[12,13] Most of these studies focus attention on the state distribution of $O(^3P_j)$ following the photodissociation of NO_2 near 225 nm.

Translational energy and angular distribution of the fragments (NO and O) have also been determined using Doppler profile measurements and velocity map ion-imaging techniques. From the study of the $O(^1D)$ Doppler profile in the photodissociation of NO_2 at 205.47 nm,[11] rotational excitation in the NO fragment is determined to be small because only a small amount of energy is released into the $O(^1D)$ atom translational degrees of freedom. Most available energy appears in the vibrational degrees of freedom for NO at 205.47 nm photodissociation. A velocity map ion-imaging study of O^+ and NO^+ by Ahmed et al.[13] at 226 nm excitation/dissociation of NO_2 finds that nearly all of the excess energy for NO_2 photodissociation into $O(^1D)$ and NO(X) appears as product translational energy;[12,13] that is, the NO(X,0) product is not highly rotationally excited. Additionally, they report that the product energy distribution is quite sensitive to the exact wavelength of the excitation/detection laser.

In a very recent paper, Richter et al.[14] discuss NO_2 fragmentation at 212.8 nm. They determine the translational energy released in the fragmentation and characterize the states of both NO and O fragments. They find that, if NO is formed in a rovibrational level that permits the formation $O(^1D)$ energetically, then this state of oxygen is the exclusive coproduct. NO_2 multiphoton processes are a factor for their experiments as well, just as we have found in the present study. They conclude that the NO from the $O(^1D)$ channel is found to be mostly in the $v'' = 3$ for 212.8 nm photodissociation.

In this present study, the dissociation of NO_2 in the region 217−237 nm is examined by probing photofragmented nascent NO using a one-laser photofragmentation/fragment-detection technique. The nascent NO spectrum changes dramatically depending on the intensity (W/cm^2) or fluence (J/cm^2) of the laser beam; the spectrum of NO becomes very crowded as the laser intensity is increased because higher rotational and vibrational levels of NO become populated. Additionally, the line width of the mass spectrum signal increases at laser wavelengths in the 227−237 nm region. This observation is interpreted as an increase in the kinetic energy of the photofragmented NO due to the multiphoton nature of the NO_2 dissociation process at high laser intensity. Near 230 nm, a spectrum is observed that cannot be attributed to NO; it has a progression in a 35 cm^{-1} energy spacing, it has multiple features with different line widths, it has an intensity pattern inconsistent with a NO rotational distribution based on a given temperature, but it is nonetheless detected in the NO mass channel. From these observations, we conclude that a higher electronic state of NO_2 has been accessed through multiphoton processes for the high laser intensity experiments. This intermediate state can be a Rydberg state, an ion-pair state ($NO^+\cdots O^-$), or other higher-electronic state of NO_2 reached by multiphoton absorption. Rotational, vibrational, and translational energy distributions of NO are estimated for the NO_2 photodissociation reaction on the basis of the observed spectra.

II. Experimental Methods

A. Apparatus and Procedures. The experimental apparatus employed for these photofragmentation studies of NO_2 has been fully described in previous papers from our laboratory.[15] NO_2 is introduced into the ionization region of a time-of-flight mass spectrometer (TOFMS) through a pulsed supersonic nozzle. A laser beam intersects the molecular beam created by this supersonic expansion at right angles to both the molecular beam flow axis and the TOFMS axis. At this intersection, NO_2 absorbs a photon (or photons) from the laser and dissociates to NO + O. The fragmented NO is subsequently probed using a $(1 + 1)$ REMPI scheme through its $A(^2\Sigma^+) \leftarrow X(^2\Pi)$ transition. NO^+ ions are detected at the end of a 1.5 m flight tube by a microchannel plate detector, and the output voltage from the detector is averaged in a boxcar averager and recorded on a computer through an ADC card.

The rovibronic excitation spectrum of fragmented NO (γ bands) is obtained by scanning the laser wavelength from 217 to 237 nm. For comparison, the (0-0) transition spectrum of NO gas itself is also recorded. Results presented below are generated by a single laser, so both NO_2 photodissociation and the NO fragment spectrum are generated by the same photons. The rotational temperature of the nascent NO is determined from simulation of the NO (0-0) band rotational spectrum using rotational spectrum simulation software for diatomic molecules developed at Sandia National Laboratory.[16] The vibrational temperature of NO-fragmented from NO_2 can be estimated based on the Franck−Condon-corrected intensity ratio $I(0\text{-}1)/I(0\text{-}0)$ and the Boltzmann population formula. The TOFMS line shape for the NO mass channel signal at a given laser wavelength is recorded on a digital oscilloscope for a 256 shot average. The full width at half-maximum (fwhm) of the feature is measured to determine the line width of the TOFMS peak at a specific NO transition. The features always appear to be symmetric. Information on the line width of this feature reflects the dissociation dynamics; in particular, it gives an estimate of the translational energy for the fragmented NO. The instrumental resolution of the TOFMS for cooled NO gas is ca. 22 ns for an unfocused beam and ca. 18 ns for a focused beam. These widths depend, in part, on the laser beam position, mode structure, and size at the ionization region of the TOFMS.

The frequency-doubled output (532 nm) of the fundamental (1064 nm) of a Nd:YAG laser is used to pump a dye laser. To obtain the required UV photons, the dye laser output is doubled and mixed with the Nd:YAG fundamental. A series of seven dyes is used to cover the fragmentation/excitation range from 237 to 217 nm: R640, R640/KR620, KR620, R610, R610/R590, R590, and R575 (Exciton). The UV output energy of this laser is between 300 and 500 μJ/pulse depending on the dye medium and exact wavelength in the output range. The laser-beam intensity is $(1.1-1.9) \times 10^5$ W/cm^2 for the unfocused beam, and for the focused beam (360 mm focal length lens), the beam intensity is $(1.3-2.1) \times 10^8$ W/cm^2. The time spread (full width at half-maximum) of this UV pulse is typically ca. 6 ns measured for the pulse envelope but this envelope typically represents a random, time-varying distribution of ca. 100 ps pulses.

NO_2 gas (99.5+% pure, Aldrich) and NO gas (98.5+% pure, Aldrich) are employed without additional purification. To suppress the reaction $NO_2 \rightarrow NO + (^1/_2)O_2$, the expansion gas for NO_2 experiments includes at least 20% O_2. A typical mixture of 0.5% NO_2, 20% O_2, and 80% (10% Ar in He), is used for these experiments. The gas mixture of $NO_2/O_2/Ar/He$ is held in a steel mixing vessel for at least 1 day to ensure thorough sample mixing. Additionally, the vessel is filled through a

Photodissociation of NO₂ in the Region 217−237 nm

J. Phys. Chem. A, Vol. 106, No. 33, 2002 **7567**

stainless steel tube plugged at one end and welded to the inlet/outlet valve at the other, which has more than 100 small holes drilled over its length. The sample gas is held in this vessel for a number of weeks over the course of these experiments to facilitate the reaction $2NO + O_2 \rightarrow 2NO_2$. The expansion gas mixture is thus thoroughly equilibrated and homogeneous before use in these experiments. This mixture is delivered through PVC or Teflon tubing to the pulsed nozzle and expanded into the vacuum chamber at a total backing pressure of 100 psig. For NO experiments (no NO₂ fragmentation), 10 ppm of NO is prepared in a premixed 10% Ar/He backing gas as indicated above.

For velocity distribution measurements, the chamber working pressure and the timing of the probe laser are kept constant and unchanged as the timing of the pulsed valve is swept. As has been reported a number of times, velocity slip occurs for these supersonic expansions of a carrier gas (He/Ar) with seeded molecules (NO₂, NO, CH₃NO₂, etc.).[17] That is, light molecular species can achieve a higher speed in the beam than the heavy ones and thereby arrive at the source region of the TOFMS earlier than the heavy ones. Thus, each molecular species in the expansion can achieve a different terminal velocity and thus a different arrival time at the ionization region of the TOFMS, depending on its mass, collision cross section, concentration, temperature, and relaxation behavior.[17] This means that each precursor species in the supersonic expansion beam has its own velocity (or arrival time) distribution at the ionization region of the time-of-flight mass spectrometer. By comparing these distributions in arrival time, one can determine the particular parent species associated with the photofragmented species as shown in ref 17 for many other molecular and cluster systems. The arrival time distribution for the observed photofragment signal can thus be related to a specific precursor molecule in the supersonic expansion by direct comparison with arrival time distributions of possible precursors. Therefore, the carrier molecule for the detected NO can be readily distinguished. Modeling of this velocity slip for NO/NO₂, employing the approximations of ref 17b, gives rough agreement with the observed arrival time differences for these species.

B. Source of NO Spectra. NO₂ is unfortunately a very complex "triatomic" molecule. It can be viewed, in general, as four systems: NO₂, (NO₂)₂(≡N₂O₄), NO, and (NO)₂. To confirm the source of the detected NO (i.e., whether it comes from the photodissociation of NO₂ or some other source or process), several different experiments and approaches have been pursued: velocity/timing measurements, comparisons of NO spectra from different samples, concentration studies, expansion gas changes, laser-intensity studies, and spectral analysis. Below, we present several results that strongly support the conclusion that the parent molecule for the photodissociation processes that we investigate is truly NO₂, that is, only photofragmented NO from NO₂ is studied in the present work.

The equilibrium constant for the reaction $NO + \frac{1}{2}O_2 \rightarrow NO_2$ is 1.3×10^9 on the basis of the Gibbs free energies for the reactants and products. In an expansion with significant cooling, the collision rate is very high at the nozzle throat in the gas phase, and therefore, an expansion with 100% O₂ at 20 psig should have a subpart per billion NO concentration. This concentration is an order of magnitude below the detection sensitivity for our experiment.[18] Therefore, the NO spectrum obtained from a sample of 0.5% NO₂/99.5% O₂ expanded at ca. 20 psi can be assumed to be derived only from NO fragmented from NO₂ and to be free of NO contamination. Additionally, the NO spectra from a partial (~20%) O₂
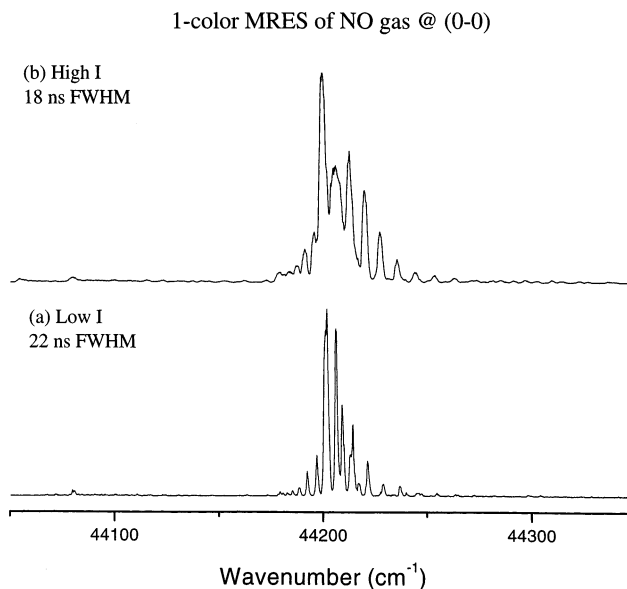

Figure 1. Mass-resolved excitation spectra (MRES) of NO gas (0.01% NO/10% Ar/90% He) at the A ← X (0-0) transition obtained using (a) low laser intensity (1.9×10^5 W/cm²) and (b) high laser intensity (2.1×10^8 W/cm²). The peak at 44 202 cm⁻¹ is the (Q₁₁ + P₂₁) band of each NO spectrum. The fwhm of the TOFMS signal for trace a is 22 ns, while that for trace b is 18 ns as indicated in the figure. Narrowing of the TOFMS line width can occur, because the interaction volume between the laser beam and NO gas becomes smaller by focusing the laser beam. Note the Stark broadening of the NO spectral features at high laser intensity.

expansion are identical to those for a full (~100%) O₂ expansion. This observation suggests that the spectra presented in this report are not associated with a NO concentration present in the sample gas prior to photodissociation of NO₂. One can compare the spectra obtained for NO that arise from two different samples: (1) a mixture of 10 ppm NO/10% Ar/90% He and (2) 0.1% NO₂ expanded with 10% Ar/90% He, 20% O₂/80% He, or 100% O₂. Such a comparison yields several observed differences. NO spectra feature Stark broadening as a function of increased laser intensity for a pure NO sample (number 1 above) but do not for a NO₂ sample (number 2 above). See Figures 1 and 2. The observed NO (0-0) rotational structure and extent do not change with increasing laser intensity for a NO sample but do change with increasing laser intensity for a NO₂ sample (see Figure 2). At the same low laser intensity and under the same expansion conditions, a NO sample gives a $T_{rot} \approx 11$ K, while a NO₂ sample gives a NO $T_{rot} \approx 30$ K (see Figure 3). At low laser intensities, the NO signal in mass channel 30 amu has a laser intensity dependence of ca. 1.5 for an expansion of 10 ppm NO/10% Ar/90% He. Under these same experimental conditions, a sample of ~0.1% NO₂/20% O₂/80% He or 0.1% NO₂/100% O₂ has a NO signal dependence on laser intensity that is greater than 2.0. Saturation effects for these two different processes (NO (1 + 1) ionization and NO₂ photodissociation/NO ionization) cause these laser energy dependences for the NO⁺ mass signal to be lower than their predicted values of 2 and 3, respectively.

As seen in Figure 4, the velocity or arrival time distribution for each NO-containing sample (1 or 2 above) is quite different. The TOFMS maximum signal in mass channel 30 (NO⁺) arrives 30 μs earlier for a NO sample than for a NO₂ sample, due to velocity slip in the supersonic molecular beam.[17] The NO (0-0) spectrum is not changed in timing for the various features for NO₂ concentrations, 0.5%, 0.1%, or 0.01%, in the expansion. All spectra are identical for these samples under the
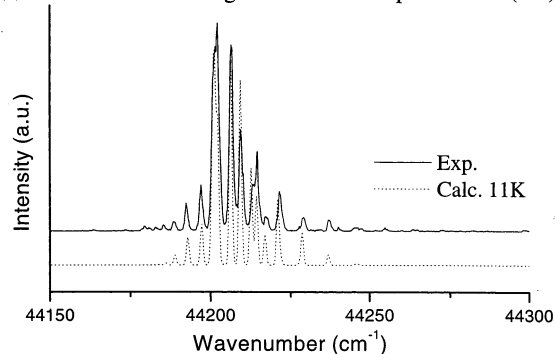
7568 *J. Phys. Chem. A, Vol. 106, No. 33, 2002*

Im and Bernstein

1-color MRES of fragmented NO
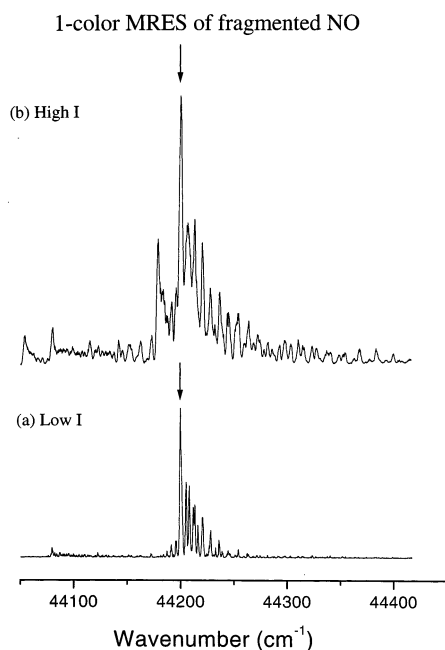
Figure 2. MRES of nascent NO from photodissociation of NO_2 obtained using (a) a low-intensity (1.9×10^5 W/cm^2) laser beam and (b) a high-intensity (2.1×10^8 W/cm^2) laser beam. The most intense peak (arrows) at 44 202 cm^{-1} is the ($Q_{11} + P_{21}$) band of each NO spectrum.
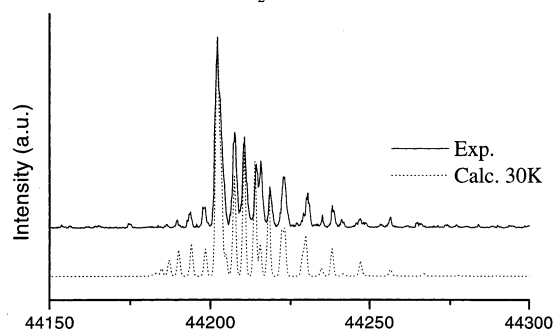
Figure 3. Simulation of the NO rotational spectrum at the (0-0) transition obtained by (a) NO gas and (b) fragmented NO from NO_2. The simulated spectrum for each sample is shown by the dotted line fit to the experimental spectrum (solid line). The rotational temperature is determined to be ~11 K for NO gas (panel a) and ~30 K for fragmented NO from NO_2.

same experimental conditions (i.e., laser intensity, expansion conditions, etc.), thereby showing that neither NO nor NO_2 complexes (($NO)_n$, $(NO_2)_n$, etc.) are involved in the NO_2 photodissociation. A final point to note is that the kinetic energy released for the photofragmented NO in our studies (see TOFMS

Velocity Slip Experiment
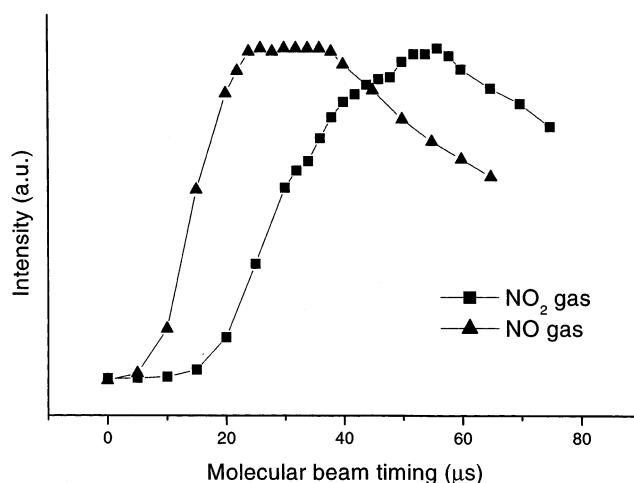
Figure 4. Velocity distributions for (▲) NO gas and (■) fragmented NO from NO_2. Both NOs are detected at mass 30.

line width measurements given below) is too small by a factor of at least 4 for the NO to arise from N_2O_4 photodissociation.[19]
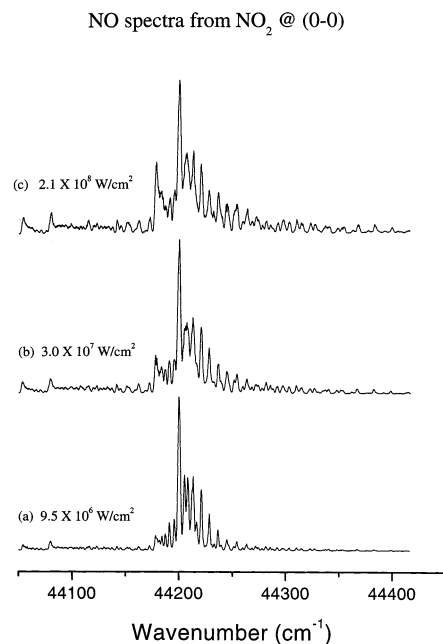
Given the above experimental observations, we conclude that the signals observed in the 30 amu (NO^+) mass channel for samples with the NO_2 parent molecule photodissociated to generate NO are derived from the isolated, cooled NO_2 molecule and not from NO, $(NO)_2$, $(NO_2)_2 (=N_2O_4)$, etc.

III. Results

The spectrum of NO from fragmented NO_2 in the NO (0-0) region of the $A(^2\Sigma^+) \leftarrow X(^2\Pi)$ transition detected in the NO^+ mass channel for two different laser intensities is presented in Figure 2. Both spectra are well-resolved, and various bands can be clearly identified in both spectra. Even though NO is fragmented from NO_2, rotationally cold NO is detected for an unfocused laser beam (Figure 2a) with 700 μJ/cm^2 fluence or ~10^5 W/cm^2 intensity. The most intense rotational feature in the spectrum, at 44 202 cm^{-1}, is assigned to the ($Q_{11} + P_{21}$) band,[20] which is the origin of this transition. The P_{11} band at 44 197 cm^{-1}, which is a hot band of the ($Q_{11} + P_{21}$) rotational transition, is considerably weaker: other bands, ($R_{11} + Q_{21}$) at 44 207 cm^{-1} and R_{21} at 44 215 cm^{-1}, are also weak. These features indicate a low rotational temperature for the fragmented NO at the $X(^2\Pi)$ $v'' = 0$ vibrational level: simulation of this rotational structure (see Figure 3) suggests a T_{rot} ca. 30 K.

On the other hand, when a focused laser beam is used to fragment NO_2 (ca. 10^8 W/cm^2 intensity or 700 mJ/cm^2 fluence), NO is born with a substantial degree of rotational excitation as shown in Figure 2b. P_{11} is now clearly much more intense and many $X(^2\Pi)$ $v'' = 0$ rotational levels are populated. In addition, significant rotational population can be observed in the $^2\Pi_{3/2}$ spin state at 120 cm^{-1} to higher energy than the $^2\Pi_{1/2}$ (X) state. The estimated rotational temperature for NO under these fluence conditions is $T_{rot} \approx 200$ K. Figure 5 shows how the rotational transition intensity (T_{rot}) increases with laser beam intensity.

The same NO (0-0) spectral pattern for a focused laser beam and a NO_2 sample can be observed for the (1-1) and (2-2) transitions as shown in Figure 6. The TOFMS line width for these peaks is the same as the high intensity (0-0) spectrum, ca. 20 ns. The (1-1) and (2-2) transitions can only be observed for a focused, high-intensity laser beam. No significant signal is observed in the (3-3) region; very weak signals, less than 10

Photodissociation of NO$_2$ in the Region 217−237 nm

J. Phys. Chem. A, Vol. 106, No. 33, 2002 **7569**

NO spectra from NO$_2$ @ (0-0)

Figure 5. (0-0) transition of fragmented NO as a function of laser intensity: (a) 9.5×10^6; (b) 3.0×10^7; (c) 2.1×10^8 W/cm^2. This observation indicates the multiphoton behavior of the spectrum.

NO from NO$_2$, High I
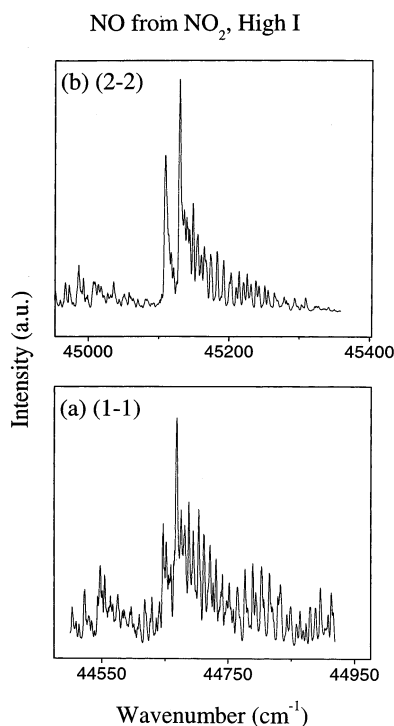
Figure 6. MRES of (a) the (1-1) transition and (b) the (2-2) transition of the nascent NO from the photodissociation of NO$_2$ obtained using high laser intensity (2.1×10^8 W/cm^2). These peaks show a fwhm of about 20 ns for a TOFMS line width. A few of them have the fwhm of about 30 ns.

mV with about a 40 ns fwhm, are found in this spectral region for the NO$^+$ mass channel.

The NO spectrum between 42 200 and 44 050 cm^{-1} has also been obtained through NO$_2$ photodissociation. These features can only be observed with a focused laser beam (high intensity). Spectra observed in the NO (2-3), (1-2), and (0-1) regions are displayed in Figure 7. The experimentally determined NO vibrational levels for both the X($^2\Pi$) ground state and the A($^2\Sigma^+$) excited state are presented in Table 1. Only the (0-1) NO

NO from NO$_2$, High I
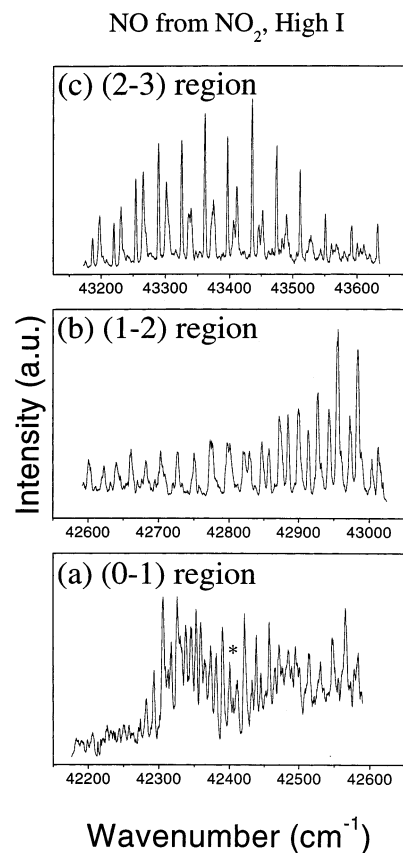
Figure 7. MRES for mass channel 30 from the photodissociation of NO$_2$ obtained using high-intensity (1.3×10^8 W/cm^2) laser excitation in (a) the (0-1) region, (b) the (1-2) region, and (c) the (2-3) region. Most of the peaks show a fwhm TOFMS line width of about 40 ns. The feature marked with ∗ in panel a has a fwhm TOFMS line width of 30 ns.

TABLE 1: The NO Vibrational Frequencies in the Ground and Excited States

vibrational level	X($^2\Pi$) (cm^{-1})	A($^2\Sigma^+$) (cm^{-1})
1	1870	2337
2	3723	4651
3[a]	5543	

[a] The energy of vibrational level 3 is obtained from ref 21.

transition is actually observed in this spectral range. Instead of observing the (1-2) and (2-3) NO transitions near 42 800 ± 200 cm^{-1} and 43 400 ± 200 cm^{-1}, respectively, much different spectra are found, consisting of doublet peaks spaced 28 cm^{-1} apart in the (1-2) region and another set of doublet peaks spaced 35 cm^{-1} apart in the (2-3) region. The NO (0-1) transition spectrum shown in Figure 7a results from rotationally hot NO because the spectrum appears similar to the one in Figure 6b for the high-intensity focused laser beam. The two other spectra of Figure 7b,c do not display any rotational bands indicative of expected NO (A ← X) transitions. The line widths of the TOFMS features for NO$^+$ (mass channel 30) generated by photofragmentation of NO$_2$ in the range 42 200−44 050 cm^{-1} are also different from those generated in the range 44 050−45 200 cm^{-1}. The NO peak just below 44 050 cm^{-1} has an associated TOFMS line width of about 40 ns, and the peak at 44 055 cm^{-1} (P$_{11}$ of $^2\Pi_{3/2}$ (0-0)) has a line width of about 20 ns, as shown in Figure 8. Most of the spectral features in the 42 200−44 050 cm^{-1} show a TOFMS peak with a line width of ca. 40 ns. Some features in the (0-1) transition region show

7570 *J. Phys. Chem. A, Vol. 106, No. 33, 2002*

Im and Bernstein

TOFMS linewidth of various NO peaks
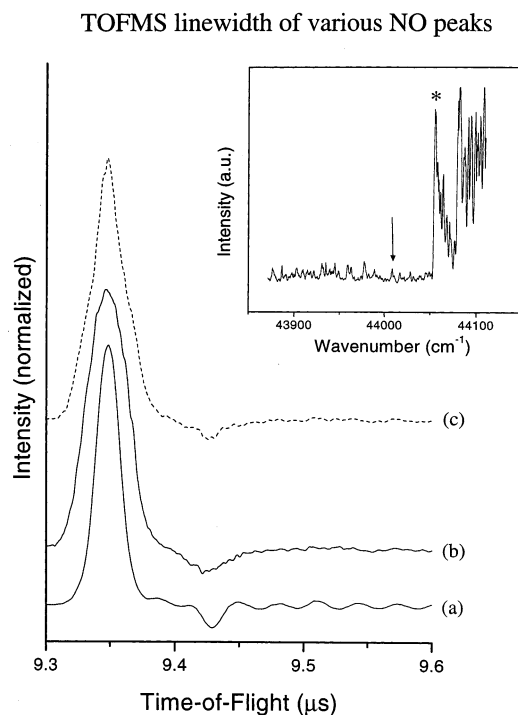
Figure 8. TOFMS line width of various NO peaks obtained with high laser intensity ($(1.3-2.1) \times 10^8$ W/cm^2). The bottom signal (trace a) is for the peak at 44 055 cm^{-1} (marked with ∗ in the inserted figure), for which fwhm is 18 ns. This peak is the lowest-energy feature in the (0-0) transition of NO. The middle trace (trace b) is for the peak at 44 008 cm^{-1} (marked with an arrow in the inserted figure), for which fwhm is 42 ns. This peak is at the high-energy end of the spectrum of trace c. The top dashed trace (trace c) is for the peak at 42 405 cm^{-1} (marked with ∗ in the inserted figure), for which fwhm is 30 ns. See the text for the details. Note that the peak in trace c has a step change in its width at roughly one-half its height.

a superposition of 40 and 20 ns line widths as presented in Figure 8c. Trace c of this figure shows a line shape not readily characterized by a single-width parameter at half-height.

IV. Discussion

A. Dissociation Mechanism for NO$_2$ near 226 nm and below. A single photon of wavelength 226 nm will excite NO$_2$ to its 2^2B_2 state. This transition ($\tilde{B}\ ^2B_2 \leftarrow \tilde{X}\ ^2A_1$) shows discrete rotational structure near its origin at ca. 249.1 nm, but the transition becomes diffuse below 245.9 nm because of vibrational predissociation.[22] At 226 nm excitation, the NO + O(^{1}D) channel for dissociation is open; the threshold for this channel is at 243.9 nm, and thus,

$$\text{NO}_2 + 1h\nu\ (226\ \text{nm}) \rightarrow \text{NO}_2^*\ (2^2B_2) \rightarrow \text{NO(X)} + \text{O}(^1\text{D})$$
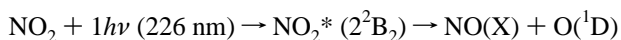
The mass-resolved excitation spectrum (MRES) of fragmented NO ca. 226 nm yields a low rotational temperature (T_{rot} ca. 30 K) with no vibrational excitation (A(0) ← X(0)). On the basis of these results, most of the excess energy for the reaction NO$_2$ + 5.480 eV ($\sim$226 nm) → NO(X) + O(^{1}D) + 0.400 eV should be released into the translational degrees of freedom of NO and O products for 226 nm photodissociation. Thus, $E(\sim$226 nm) = 5.480 eV = 5.08 eV + 0.005 eV ($T_{\text{rot}} \approx 30$ K) + 0.137 eV + 0.257 eV = $E_{\text{diss}} + E_{\text{rot}} + E_{\text{trans}}(\text{NO}) + E_{\text{trans}}(\text{O})$. This translational energy distribution for both NO and O(^{1}D) has been observed by velocity map ion-imaging studies recently reported.[12,13] If $v'' = 1$ were populated under these conditions of low laser intensity, the NO and O(^{1}D) rotational and translational

energy distributions would need to be much different than observed. The amount of translational energy available to NO under these conditions is insufficient for fragmented NO in this process to occupy the $v'' = 1$ vibrational level at 1870 cm^{-1} (see Table 1). This is the reason that with the unfocused laser beam (low intensity to ensure only single-photon NO$_2$ excitation, $\tilde{B} \leftarrow \tilde{X}$), only the (0-0) NO A($^2\Sigma^+$) ← X($^2\Pi$) transition is observed. These observations are consistent with the NO$_2$ molecule dissociating from a linear configuration on a repulsive part of the potential surface.

The additional kinetic energy for photofragmented NO means that the NO ion has an additional velocity that either assists or hinders the acceleration given the ion by the ca. 250 V/cm electric field in the ion extraction region (4000−3750 V) of the TOFMS ion source. This additional NO kinetic energy from NO$_2$ photofragmentation should generate an additional TOFMS line width for the 30 amu (NO$^+$) mass channel signal. Employing the TOFMS equations for the ion flight time,[23] we calculate the TOFMS signal line width for the NO$^+$ photofragment with $E_{\text{trans}}(\text{NO}) = 0.137$ eV kinetic energy to be ca. 20 ns. This line width is comparable to the instrumental line width.

When the photolysis/probe beam is focused ($\sim$10^8 W/cm^2), the (0-0), (1-1), and (2-2) vibronic transitions of NO A ← X are observed with an extensive rotational structure (T_{rot} ca. 200 K) as shown in Figures 5 and 6. Spectra in these figures can only be observed with high-intensity laser excitation.

The focused laser beam produces a much more highly excited NO (both rotationally and vibrationally) than does the unfocused beam. This circumstance implies more excess energy in NO$_2$ for the focused beam than for the unfocused beam photolysis conditions. Note that from the above energy balance discussion, single-photon excitation of NO$_2$ to the $\tilde{B}$ state in this energy region (44 200 cm^{-1}, (0-0) transition for NO A ← X) is not energetic enough to dissipate more energy into vibrational and rotational degrees of freedom with O(^{1}D) production. Thus, multiphoton excitation of NO$_2$ must occur to generate the required NO energy balance and summation. The (0-0) NO structure of Figure 5 clearly shows a laser-intensity dependence: a multiphoton process for NO$_2$ photodissociation is indicated. Under single-photon NO$_2$ excitation to the $\tilde{B}$ state, the excess energy is not sufficient for X ($v'' = 2$) occupation if O(^{1}D) is also produced. If one assumes that the dissociation occurs through production of O(^{3}P) ground state, then (3-3) should also be observed: no (3-3) (ca. 45 700 cm^{-1} or 219 nm) could be detected for a focused laser beam in the appropriate spectral region. These arguments lead to the conclusion that NO production for focused and unfocused laser beam excitation of NO$_2$ is through different pathways.

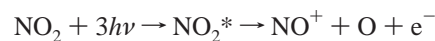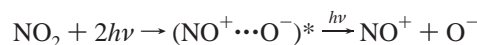From laser intensity studies, the fragmentation of NO$_2$ and the excitation and ionization of NO (for the (0-0), (1-1), and (2-2) NO A ← X transitions) require four or more photons: at least two to excite the NO$_2$ and two to excite the NO(X) photoproduct. Saturation for the second photon absorbed for NO$_2$ or for NO or for both probably occurs. A two-photon dissociation of NO$_2$ puts about 11 eV into NO$_2$. Two possible excited states of NO$_2$ in the 11 eV region can be suggested as candidates for the NO$_2$ dissociative states reached at high laser intensity (i.e., by two-photon absorption in the 226−200 nm region): a Rydberg state at 10.85 eV and an ion-pair state (NO$^+\cdots$O$^-$). The energy of the ion-pair state ($E_{\text{NO}^+\text{O}^-}$) can be estimated as follows:[25]

$$E_{\text{NO}^+\text{O}^-} = D_0(\text{ON}-\text{O}) + \text{IP}(\text{NO}) - \text{EA}(\text{O})$$

in which D_0 is the dissociation energy of NO_2 to NO + O, IP(NO) is the ionization energy of NO, and EA(O) is the electron affinity of O. This equation gives 10.92 eV for the threshold of the NO_2 ion-pair state. Thus, NO_2 with the absorption of two photons at ca. 225 nm ($\sim$11 eV) can be excited to either a Rydberg state or an ion-pair state. For either state, the dissociation dynamics can produce NO(X) predominantly, $NO_2 + 2h\nu \rightarrow NO_2^* \rightarrow NO(X) + O$. NO(X) must be generated because the (0-0), (1-1), and (2-2) transitions of the NO A ← X transition are detected. An energy balance must be achieved through oxygen atom excitation for this 226−220 nm excitation of NO_2 and probe of NO.

B. Dissociation Mechanisms for NO_2 between 237 and 227 nm. The fragmentation of NO_2 by excitation in the region 237−227 nm (42 195−44 050 cm^{-1}, A ← X (0-1), (1-2), (2-3), Figure 7) is different than that described above for the region 226−220 nm (A ← X (0-0), (1-1), (2-2)) on the basis of both literature reports[9] and the present studies. First, most features in the spectral range 227−237 nm generate a TOFMS line width for the NO^+ signal of about 40 ns. This value is twice that observed for the high-intensity laser studies below 226 nm and that observed for the low-intensity A ← X (0-0) NO transition. Second, in the range 231−233 nm, doublet peaks with 28 cm^{-1} spacings are observed (Figure 7b), and at 230 nm (Figure 7c), these spacings become 35 cm^{-1} and the spectrum seems to consist of a few different vibronic progressions. These two observations lead us to conclude that these spectra do not arise from NO excitation but rather that these features are NO_2 transition peaks that are detected in the NO mass channel. NO dissociates from NO_2 after the resonance in the NO_2 vibronic energy levels accessed in a multiphoton process. Results from other studies[9] and our NO gas-phase experiments support this conclusion: no NO features are observed around the expected NO (1-2) and (2-3) transitions. We have attempted to fit these spacings to transitions involving two NO or NO_2 excited electronic states and to generate such spectral spacing using a two-color excitation scheme for both NO and NO_2. We are not able to fit the observed pattern of transitions, employing known states of either molecule. Note, however, that in the (0-1) region, both NO and NO_2 features appear. The TOFMS line width for the 227−237 nm region gives a much larger kinetic energy for the NO fragment than that found in the 227−220 nm region. The TOFMS instrumental resolution is approximately 20 ns at mass channel 30 amu, and NO^+ signals with larger line widths than this should arise from photofragmented NO with additional kinetic energy due to NO_2 fragmentation. The kinetic energy of NO generated by NO_2 photodissociation in the 237−230 nm region is $\sim$0.4 ± 0.04 eV; this gives a NO velocity of $\sim$1600 m/s in the direction of the electric vector (parallel to the flight tube axis) of the laser beam (a 40 ns line width for the TOFMS feature). Because no signal in this region is observed for an unfocused beam, we conclude that the excited electronic state from which NO_2 dissociates must be accessed by two- or three-photon excitation in this wavelength region (227−237 nm).

Three possible pathways (NO_2 excited electronic states from which dissociation occurs) can be suggested that would lead to these NO_2-related spectra detected in the NO mass channel: (1) NO^+ can be produced through a NO_2 ion-pair state, as discussed above; (2) neutral NO fragments can be produced in a highly excited electronic state through NO_2 multiphoton absorption and can be ionized subsequently by one-photon absorption, as reported in a previous study;[26] (3) NO^+ can be produced through the accessible NO_2 excited states during NO_2 dissociation. Explicitly,

$$NO_2 + 2h\nu \rightarrow (NO^+ \cdots O^-)^* \xrightarrow{h\nu} NO^+ + O^-$$

$$NO_2 + 3h\nu \rightarrow NO_2^* \rightarrow NO^* + O \xrightarrow{h\nu} NO^+ + O + e^-$$

$$NO_2 + 3h\nu \rightarrow NO_2^* \rightarrow NO^+ + O + e^-$$

The production of NO^+ from NO_2 requires at least 12.4 eV (D_0(ON−O) + IP(NO)) of energy deposited in the NO/NO_2 system. The two-photon energy available in the wavelength region 230−237 nm is less than 10.9 eV and thus is not high enough to produce NO^+ through NO_2 dissociation directly: to produce NO^+ from NO_2 dissociation, the pathway should involve absorption of at least three photons. Thus, the two NO_2 to NO^+ mechanisms require three photons absorbed by NO_2 with a resonance at the second or third absorption steps. Generation of electronically excited neutral NO can occur through a three-photon NO_2 absorption with resonance and final ionization of NO by an additional photon absorption.

In the region of the (0-1) NO transition (235−237 nm), both NO A ← X (0-1) features and NO_2 multiphoton resonances are observed (see Figure 7a). The TOFMS line width in this (0-1) region is a composite of 20 and 40 ns widths (see Figure 8c). These observations imply that NO is generated at these wavelengths by two parallel mechanisms, one producing NO(X) and one producing electronically excited NO or directly NO^+, with resonant NO_2 absorptions.

The main point of the above discussion of the photodissociation of NO_2 between 237 and 217 nm is that the process does not simply involve the B̃ (2^2B_2) state of NO_2 accessed by a single photon present in this wavelength region. The NO_2 behavior is demonstrably quite complex, depending on both the single-photon energy and the number of photons present in the active volume for NO_2 absorption. This combination yields both NO and NO_2 spectra in the region 237−217 nm that are laser-intensity-dependent.

V. Conclusions and Summary

Photodissociation of NO_2 is studied by detection of MRES of NO and by observation of resonances in the NO_2 multiphoton excitation process also detected in the NO^+ mass channel. Possible dissociation pathways are suggested for this complex photodissociation that depend on the experimental conditions, in particular, the laser intensity and laser pump/probe wavelength. The intensity of the laser beam (focused vs unfocused) has a major impact on the spectra and TOFMS line width detected in the spectral region 237−217 nm. Some general conclusions can be stated as follows:

(1) Single-photon dissociation of NO_2 through the 2^2B_2 state occurs (low laser intensity) to produce NO(X) at low rotational and vibrational excitation [A($^2\Sigma^+$, $\nu' = 0$) ← X($^2\Pi$, $\nu'' = 0$)] with NO kinetic energy of ca. 0.137 eV.

(2) Multiphoton dissociation of NO_2 through a Rydberg excited state or an ion-pair state occurs to produce translationally, rotationally, and vibrationally hot NO [T_{rot} ca. 200 K, A($^2\Sigma^+$, $\nu'' = 0, 1, 2$) ← X($^2\Pi$, $\nu'' = 0, 1, 2$)]. For NO_2 multiphoton dissociation, both neutral and ionic NO can be produced.

(a) In the range 220−227 nm, mostly neutral NO fragments are detected through NO (A ← X) transitions with an instrument resolution limited 20 ns NO^+ mass channel line width consistent with a NO kinetic energy of ca. 0.137 ± 0.01 eV (935 m/s).

(b) In the range 227−235 nm, ionic and electronically excited NO fragments are detected that are probably generated through

a NO_2 Rydberg or ion-pair state. This mechanism generates a TOFMS line width of 40 ns corresponding to a NO^+ kinetic energy of 0.4 ± 0.04 eV (1600 m/s). Spectra detected in the NO^+ mass channel in this wavelength range reflect resonances in the NO_2 multiphoton excitation.

(c) In the region of 235−237 nm, a mixture of these latter two mechanisms for NO_2 photodissociation can occur and a complex spectrum in the NO $[A(v' = 0) \leftarrow X(v'' = 1)]$ region is observed, composed of both NO (0-1) and NO_2 transitions.

References and Notes

(1) (a) Haller, E.; Koeppel, H.; Cederbaum, L. S. *J. Mol. Spectrosc.* **1985**, *111*, 377. (b) Bigio, L.; Grant, E. R. *J. Chem. Phys.* **1987**, *87*, 5589. (c) Knickelbein, M. B.; Haber, K. S.; Bigio, L.; Grant, E. R. *Chem. Phys. Lett.* **1986**, *131*, 51. (d) Haber, K. S.; Wiedmann, R. T.; Campos, F. X.; Zwanziger, J. W.; Grant, E. R. *Chem. Phys.* **1989**, *129*, 73. (e) Zhao, X. Z.; Lu, T. X.; Cui, Z. F. *Chem. Phys. Lett.* **1989**, *159*, 37. (f) Georges, R.; Delon, A.; Jost, R. *J. Chem. Phys.* **1995**, *103*, 1732.

(2) (a) Toselli, B. M.; Barker, J. R. *J. Chem. Phys.* **1989**, *91*, 2239. (b) Suzuki, T.; Hradil, V. P.; Hewitt, S.; Houston, P. L.; Whitaker, B. J. *Chem. Phys. Lett.* **1991**, *187*, 257. (c) Robie, D. C.; Hunter, M.; Bates, J. L.; Reisler, H. *Chem. Phys. Lett.* **1992**, *193*, 413 and references therein. (d) Brucker, G. A.; Ionov, S. I.; Chen, Y.; Wittig, C. *Chem. Phys. Lett.* **1992**, *194*, 301. (e) Changlong, N.; Hua, L.; Pfab, J. *J. Phys. Chem.* **1993**, *97*, 7458. (f) Ionov, S. I.; Brucker, G. A.; Jaques, C.; Chen, Y.; Wittig, C. *J. Chem. Phys.* **1993**, *99*, 3420. (g) Bezel, I.; Stolyarov, D.; Wittig, C. *J. Phys. Chem. A* **1999**, *103*, 10268. (h) Bezel, I.; Ionov, P.; Wittig, C. *J. Chem. Phys.* **1999**, *111*, 9267.

(3) Kawasaki, M.; Sato, H.; Fukuroda, A.; Kikuchi, T.; Kobayashi, S.; Arikawa, T. *J. Chem. Phys.* **1987**, *86*, 4431.

(4) (a) Radhadkrishnan, G.; Ng, D.; Estler, R. C. *Chem. Phys. Lett.* **1981**, *84*, 260. (b) Mons, M.; Dimicoli, I. *Chem. Phys. Lett.* **1986**, *131*, 298.

(5) (a) Slanger, T. G.; Bischel, W. K.; Dyer, M. J. *J. Chem. Phys.* **1983**, *79*, 2231. (b) McFarlane, M.; Polanyi, J. C.; Shapter, J. G. *J. Photochem. Photobiol. A: Chem.* **1991**, *58*, 139.

(6) Singhal, R. P.; Kilic, H. S.; Ledingham, K. W. D.; Kosmidis, C.; McCanny, T.; Langley, A. J.; Shaikh, W. *Chem. Phys. Lett.* **1996**, *253*, 81.

(7) Morrison, R. J. S.; Grant, E. R. *J. Chem. Phys.* **1982**, *77*, 5994.

(8) Bigio, L.; Tapper, R. S.; Grant, E. R. *J. Phys. Chem.* **1984**, *88*, 1271.

(9) Marshall, A.; Clark, A.; Ledingham, K. W. D.; Sander, J.; Singhal, R. P. *Int. J. Mass Spectrom. Ion Processes* **1993**, *125*, R21.

(10) (a) Ruban, H.-G.; van der Zande, W. J.; Zhang, R.; Bronikowski, M. J.; Zare, R. N. *Chem. Phys. Lett.* **1991**, *186*, 154. (b) Miyawaki, J.; Tsuchizawa, T.; Yamanouchi, K.; Tsuchiya, S. *Chem. Phys. Lett.* **1990**, *165*, 168. (c) Huang, Y.-L.; Gordon, R. J. *J. Chem. Phys.* **1992**, *97*, 6363.

(11) Shafer, N.; Tonokyra, K.; Matsumi, Y.; Tasaki, S.; Kawasaki, M. *J. Chem. Phys.* **1991**, *95*, 6218.

(12) Ahmed, M.; Peterka, D. S.; Bracker, A. S.; Vasyutinskii, O. S.; Suits, A. G. *J. Chem. Phys.* **1999**, *110*, 4115.

(13) Ahmed, M.; Peterka, D. S.; Suits, A. G. In *Atomic and Molecular Beams. The State of the Art 2000*; Compargue, R., Ed.; Springer: New York, 2001; p 343.

(14) Richter, R. C.; Khamaganov, V. I.; Hynes, A. J. *Chem. Phys. Lett.* **2000**, *319*, 341.

(15) Bernstein, E. R.; Law, K.; Schauer, M. *J. Chem. Phys.* **1984**, *80*, 207.

(16) Breiland, W. G. *ROT.CALC*. Sandia National Labs: Albuquerque, NM, 1992.

(17) (a) Shang, Q. Y.; Moreno, P. O.; Li, S.; Bernstein, E. R. *J. Chem. Phys.* **1993**, *98*, 1876. (b) DePaul, S.; Pullman, D.; Friedrich, B. *J. Phys. Chem.* **1993**, *97*, 2167. (c) Li, S.; Bernstein, E. R. *J. Chem. Phys.* **1992**, *97*, 792.

(18) Lemire, G. W.; Simeonsson, J. B.; Sausa, R. C. *Anal. Chem.* **1993**, *65*, 529.

(19) (a) Mueller, J.; Morton, M. L.; Curry, S. L.; Abbatt, J. P. D.; Butler, L. J. *J. Phys. Chem. A* **2000**, *104*, 4825. (b) Parsons, B. F.; Curry, S. L.; Mueller, J. A.; Ray, P. C.; Butler, L. J. *J. Chem. Phys.* **1999**, *111*, 8486. (c) Sisk, W. N.; Miller, C. E.; Johnston, H. S. *J. Phys. Chem.* **1993**, *97*, 9916. (d) Kawasaki, M.; Kasatani, K.; Sato, H.; Shinohara, H.; Nishi, N. *Chem. Phys.* **1983**, *78*, 65. (e) Inoue, G.; Nakata, Y.; Usui, Y.; Akimoto, H.; Okuda, M. *J. Chem. Phys.* **1979**, *70*, 3689.

(20) (a) Hippler, M.; Pfab, J. *Chem. Phys. Lett.* **1995**, *243*, 500. (b) Herzberg, G. In *Spectra of Diatomic Molecules*; Van Nostrand: New York, 1950; p 257.

(21) Im, H.-S.; Bernstein, E. R. *J. Chem. Phys.* **2000**, *113*, 7911.

(22) (a) VanDaele, A. C.; Hermans, C.; Simon, P. C.; Carleer, M.; Coli, R.; Fally, S.; Merienne, M. F.; Jenouvrier, A.; Coquart, B. *J. Quant. Spectrosc. Radiat. Transfer* **1998**, *59*, 171. (b) Uselman, W. M.; Lee, E. K. C. *Chem. Phys. Lett.* **1975**, *30*, 212. (c) Harris, L.; King, G. W.; Benedict, W. S.; Pearse, R. W. B. *J. Chem. Phys.* **1940**, *8*, 765.

(23) Choi, Y.-K.; Im, H.-S.; Jung, K.-W. *Int. J. Mass Spectrom.* **1999**, *189*, 115.

(24) (a) Shiell, R. C.; Hu, X. K.; Hu, Q. J.; Hepburn, J. W. *J. Phys. Chem. A* **2000**, *104*, 4339. (b) Martin, J. D. D.; Hepburn, J. W. *Phys. Rev. Lett.* **1997**, *79*, 3154.

(25) Martin, J. D. D.; Hepburn, J. W. *J. Chem. Phys.* **1998**, *109*, 8139.

(26) Davies, J. A.; LeClaire, J. E.; Continetti, R. E.; Hayden, C. C. *J. Chem. Phys.* **1999**, *111*, 1.